

3

Calibration of the Ordovician Timescale

Peter M. Sadler and Roger A. Cooper

Ordovician deep-water shales contain the prerequisites for a high-resolution timescale: rich successions of graptolite faunas, datable ash-fall K-bentonites, and minimally interrupted accumulation. Traditionally, the first appearances of selected graptolite taxa define provincial sets of zones, into which radiometrically dated bentonites are subsequently arrayed to achieve a numerical timescale. Provincial differences and the modest numbers of zones impose the primary limits on resolution. We have taken a different approach that avoids the constraint of zones.

■ The New Approach

To achieve a unifying timescale for this book, we applied computer-assisted optimization to combine graptolite range charts from all provinces directly, without using zones. The optimization process searches for a model sequence of all range-end events that best fits all the locally observed taxon ranges. Dated ash-fall events are included with the range-end events from the outset of the search; thus, they too receive optimal placements in the model sequence and permit numerical ages for biostratigraphic events to be estimated by interpolation. By this method, we interpolated ages for the Australasian graptolite zone boundaries (VandenBerg and Cooper 1992). Ages for the boundaries in other subdivision schemes were

derived, using all available criteria to correlate into the Australasian graptolite zonation (chapter 2).

■ The Raw Data

The timescale is based on an ordered and scaled sequence of 2,306 events: 22 dated bentonites that are associated with graptolites or other fossils for which contemporary graptolites are known (table 3.1); 12 undated bentonite beds that help tie together short sections from the Mohawk Valley (C. E. Mitchell pers. comm.); and the first and last appearances of 1,136 taxa (1,119 graptolites, plus 17 trilobites and conodonts) as reported from almost 200 stratigraphic range charts worldwide, from the basal Ordovician to early Devonian. The range charts represent Arctic (31), Cordilleran (10), Midwestern (6), and North-eastern (29) North America, as well as South America (9), Great Britain (24), Iberia (9), Germany (10), Scandinavia (16), eastern Europe (14), the Middle East to Central Asia (14), Siberia (1), China (16), and Australasia (9). These are all the range charts we could find that meet modern standards of graptolite systematics and depict collections from shaley facies. Inclusion of Silurian range charts and radiometric dates permits a more robust calibration. Cambro-Ordovician trilobite and conodont taxa were added to improve the constraints near the base of the Or-

TABLE 3.1. Radiometric Control Points

Age (Ma)		Unit	Stratigraphic Constraint	Reference	
491 ± 1	[U-Pb]	Latest Cambrian	<i>Peltura scarabaeoides scarabaeoides</i>	Davidek et al. 1998	
489 ± 0.6	[U-Pb]	Cambrian/Ordovician	<i>Peltura scarabaeoides scarabaeoides</i>	Landing et al. 2000	
483 ± 1	[U-Pb]	Late Tremadocian	<i>Hunnegraptus</i> sp.	Landing et al. 1997	
469 +5 -3	[U-Pb]	Arenig/Llanvirn	<i>Undulograptus austrodentatus</i>	Tucker & McKerrow 1995	(12)
465.7 ± 2.1	[U-Pb]	Llanvirn	above <i>Didymograptus artus</i>	"	(13)
464 ± 2	[U-Pb]	Llanvirn	[Cerro Viejo section—Argentina]	Huff et al. 1997; Mitchell et al. 1998	
464.6 ± 1.8	[U-Pb]	Llanvirn	<i>Holmograptus spinosus</i>	Tucker & McKerrow 1995	(14)
			<i>Didymograptus murchisoni</i>		
460.4 ± 2.2	[U-Pb]	Llanvirn	<i>Pterograptus elegans</i>	"	(15)
			<i>Hustedograptus teretiusculus</i>		
455 ± 3	[Ar-Ar]	"Kinnekulle" K-bentonite	<i>Climacograptus bicornis</i>	"	(18)
			<i>Climacograptus wilsoni</i>		
456.9 ± 1.8	[U-Pb]	"Kinnekulle" K-bentonite	<i>Climacograptus bicornis</i>	"	(18)
			<i>Climacograptus wilsoni</i>		
454.8 ± 1.7	[U-Pb]	"Pont-y-ceunant ash"	<i>Dicranograptus clingani</i>	"	(19)
			<i>Diplograptus foliaceus</i>		
457.4 ± 2.2	[U-Pb]	"Pont-y-ceunant ash"	<i>Dicranograptus clingani</i>	"	(19)
			<i>Diplograptus foliaceus</i>		
453.1 ± 1.3	[U-Pb]	"Millbrig" K-bentonite	<i>Climacograptus bicornis</i>	"	(20a)
			<i>Ensignraptus caudatus</i>		
454.1 ± 2.1	[Ar-Ar]	"Millbrig" K-bentonite	<i>Climacograptus bicornis</i>	Kunk et al. 1985; Tucker & McKerrow 1995	(20a)
			<i>Ensignraptus caudatus</i>		
454.5 ± 0.5	[U-Pb]	"Deicke" K-bentonite	<i>Climacograptus bicornis</i>	Tucker & McKerrow 1995	(20b)
			<i>Ensignraptus caudatus</i>		
445.7 ± 2.4	[U-Pb]	Ashgill	[Dobs Linn section—UK]	"	(21)
438.7 ± 2.1	[U-Pb]	Llandovery	[Dobs Linn section—UK]	"	(22)
436.2 ± 5.0	[Ar-Ar]	Llandovery	<i>Coronograptus cyphus</i>	"	(23)
430.1 ± 2.4	[U-Pb]	Llandovery/Wenlock	<i>Oktavites spiralis</i>	"	(24)
423.7 ± 1.7	[Ar-Ar]	Ludlow	<i>Lobograptus scanicus</i>	Kunk et al. 1985	
421.0 ± 2	[K-Ar]	Ludlow	<i>Neodiversograptus nilssoni</i>	Tucker & McKerrow 1995	(25)
417.6 ± 1.0	[U-Pb]	Lochkovian	<i>Monograptus uniformis</i>	Tucker et al. 1998	

Note: The "stratigraphic constraint" column names the local range chart in which the dated bed can be placed or the taxon used to constrain an isolated bed in the optimal sequence. *P. s. scarabaeoides* is a trilobite; all other listed taxa are graptolites. "Sensitive High Resolution Ion Microprobe" (SHRIMP) dates (Compston and Williams 1992) were avoided pending resolution of systematic differences from the isotope dilution dates and questions about analytical standards. The entries "U-Pb" and "Ar-Ar" distinguish dates determined by the uranium-lead and argon-argon methods, respectively.

dovician, where graptolite species richness is very low. Because habitats and fossil preservation are patchy, the local range charts disagree in detail concerning the sequence of first and last appearances of taxa. The rules for resolving these discrepancies are straightforward, but the data set is so large that computer assistance is essential.

■ Computer-Assisted Calibration

Optimization algorithms in the CONOP9 software (Kemple et al. 1995; Sadler 2001) proceed by iterative improvement from an initially randomized sequence of events toward a "best-fit" sequence. They arrive at a model sequence for all 2,306 events with the best-known fit to the field observations in the sense that a minimum of stratigraphic range extensions is required to fit every local range chart to the model. The means of measuring the length of range extensions is critical to the outcome of the opti-

mization. For this calibration task, we minimized the number of other range ends overlapped by the extensions, not the stratigraphic thickness of the extensions as minimized in graphic correlation techniques. This change eliminates bias due to variations in accumulation rate and favors those sequences preserved in the most richly fossiliferous sections. Such a misfit measure can solve ordinary correlation problems in which all sections span approximately the same time interval. It needs augmentation here because the local sections span only small fractions of the total time interval. We ensure that local sections are "stacked" in the correct order by simultaneously minimizing a second component of misfit borrowed from unitary association techniques (Guex 1991; Alroy 1992). The additional term counts the number of coexistences of pairs of taxa that are implied by the model sequence but not observed anywhere. The outcome of searching on these two criteria is an optimally ordered sequence of events.

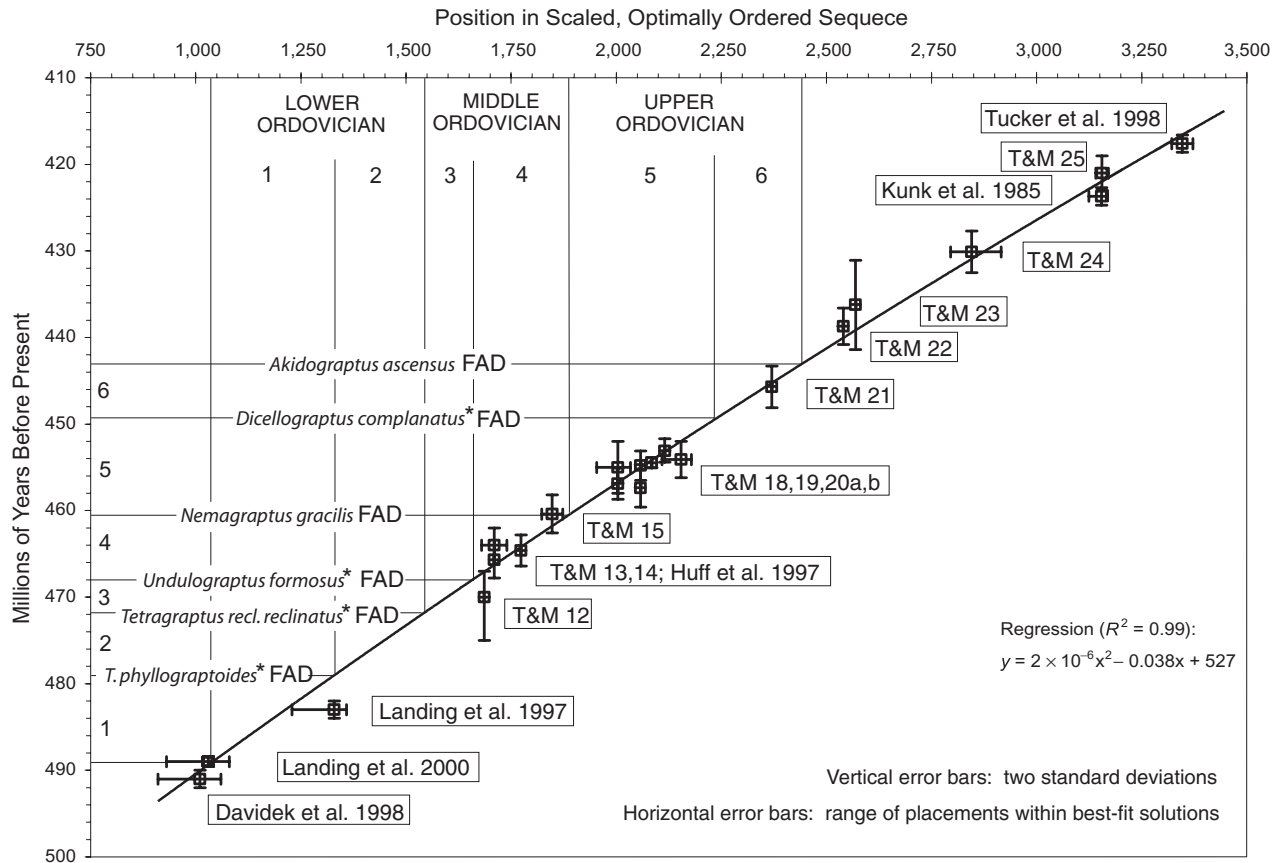


FIGURE 3.1. A projection of the six numbered chronostratigraphic time-slice boundaries, as used in this book, from the scaled optimally ordered sequence into the numerical timescale, by regression on the optimal placements of dated ash-fall events. We use, somewhat arbitrarily, a very small second-order polynomial term and force the line through the high-quality Cambro-Ordovician date. Similar results can be achieved with cubic splines (Frits Agterberg pers. comm.) or the locally estimated sum of squares. T&M refers to numbered dated items in Tucker and McKerrow (1995), many of them from Tucker et al. (1990).

Biostratigraphic field observations alone support the optimal *sequence*, but severe simplifying assumptions are unavoidable for scaling the time *intervals* between events. Two explicit simplifications were chosen as the least objectionable: in the long term, net taxonomic change (numbers of first- and last-appearance events) is a guide to the relative duration of whole sections; in the short term, stratigraphic thickness is a better guide to relative duration, especially in deep-water shales. The scaling assumptions are applied as follows. First, all local range charts are adjusted to fit the optimal sequence: observed taxon ranges are extended, if necessary, and missing taxa are inserted. Second, the total thickness of each section is rescaled according to the fraction of the composite sequence that it spans. Third, the spacing of adjacent events in the best-fit composite sequence is set equal to the average of all the local rescaled spacings. Zero

values are included in the average to allow for mass extinctions and rapid radiations. The result at this stage is a relative timescale—a scaled, optimally ordered sequence in which events are spaced in proportion to one possible approximation of their separation in time.

■ Tests of the Calibration

The ultimate test of the scaling process plots the position of the dated events in the putative relative timescale against their radiometric ages on a regular numeric timescale. The near-linear regression in figure 3.1 justifies the scaled, optimally ordered sequence as a *plausible* proxy for a timescale and therefore suitable for interpolating the age of traditional zone boundaries. This regression test was actually applied in three stages. The first stage omitted the Australasian composite sec-

tion (VandenBerg and Cooper 1992) and used only the 607 taxa observed in more than one non-Australasian section; the second stage added Australasian ranges; the third stage (figure 3.1) added those taxa known from only a single section. The fit to a linear regression improved slightly with each step. Because of provincial differences, presumably aggravated by the difficulty of achieving perfect optimization for huge data sets, the ordinal regression between our optimally ordered sequence and the Australasian sequence is not perfect, but it has a high correlation coefficient. Australasian zone boundaries were placed in the spaced, optimally

ordered sequence at the first appearance of a cluster of zonal taxa (usually three to four). If this level did not coincide with the appearance of the customary defining species, a substitute species was selected from the cluster (asterisks in figure 3.1).

ACKNOWLEDGMENTS

This work was supported in part by National Science Foundation grant EAR 9980372 to Sadler. Fritz Agterberg, Barry Webby, and Henry Williams suggested improvements on an earlier draft.